# *Microfluidic separation of canine adipose-derived mesenchymal stromal cells*



**Citation:** Liu, Zhuoming, Screven, Rudell, Yu, Debbie, Boxer, Lynne, Myers, Michael J et al. 2021. "Microfluidic separation of canine adipose-derived mesenchymal stromal cells." Tissue Engineering Part C Methods, 27 (8).

**As Published:** 10.1089/TEN.TEC.2021.0082

**Publisher:** Mary Ann Liebert Inc

**Persistent URL:** https://hdl.handle.net/1721.1/143613

**Version:** Final published version: final published article, as it appeared in a journal, conference proceedings, or other formally published context

TISSUE ENGINEERING: Part C
Volume 27, Number 8, 2021

DOI: 10.1089/ten.tec.2021.0082

termis
Tissue Engineering
& Regenerative Medicine
International Society

***METHODS ARTICLE***

# Microfluidic Separation of Canine Adipose-Derived Mesenchymal Stromal Cells

Zhuoming Liu, PhD,[1] Rudell Screven, MS,[1] Debbie Yu, PhD,[2] Lynne Boxer, DVM,[3] Michael J. Myers, PhD,[1] Jongyoon Han, PhD,[2] and Laxminarayana R. Devireddy, DVM, PhD[1]



Mesenchymal stromal cells (MSCs) are potential treatments for a variety of veterinary medical conditions. However, clinical trials have often fallen short of expectations, due in part to heterogeneity and lack of characterization of the MSCs. Identification and characterization of subpopulations within MSC cultures may improve those outcomes. Therefore, the functional heterogeneity of different-sized subpopulations of MSCs was evaluated. A high-throughput, biophysical, label-free microfluidic sorting approach was used to separate subpopulations of canine adipose-derived MSCs (Ad-MSCs) based on size for subsequent characterization, as well as to evaluate the impact of culture conditions on their functional heterogeneity. We found that culture-expanded canine Ad-MSCs comprise distinct subpopulations: larger MSCs (mean diameter of $18.6 \pm 0.2$ μm), smaller MSCs (mean diameter of $15.3 \pm 0.2$ μm), and intermediate MSCs (mean diameter of $16.9 \pm 0.1$ μm). In addition, proliferation characteristics, senescence, and differentiation potential of canine Ad-MSCs are also dependent on cell size. We observed that larger MSCs proliferate more slowly, senesce at earlier passages, and are inclined to differentiate into adipocytes compared with smaller MSCs. Most importantly, these size-dependent functions are also affected by the presence of serum in the culture medium, as well as time in culture. Cell surface staining for MSC-specific CD44 and CD90 antigens showed that all subpopulations of MSCs are indistinguishable, suggesting that this criterion is not relevant to define subpopulations of MSCs. Finally, transcriptome analysis showed differential gene expression between larger and smaller subpopulations of MSCs. Larger MSCs expressed genes involved in cellular senescence such as cyclin-dependent kinase inhibitor 1A and smaller MSCs expressed genes that promote cell growth [mechanistic target of rapamycin 1 (mTORC1) pathway] and cell proliferation [myelocytomatosis (*myc*), *e2f* targets]. These results suggest that different subpopulations of MSCs have specific properties.

**Keywords:** microfluidics, cell size, multipotentiality

### Impact Statement

Clinical trials of mesenchymal stromal cells (MSCs) from veterinary species have often fallen short of expectations, due in part to heterogeneity and lack of characterization of the MSCs. A high-throughput, biophysical, label-free microfluidic sorting approach was used to separate subpopulations of canine adipose-derived MSCs (Ad-MSCs) based on size for subsequent characterization. Proliferation characteristics, senescence, and differentiation potential of canine Ad-MSCs are also dependent on cell size. Cell surface staining for MSC-specific cell surface markers showed that all subpopulations of MSCs are indistinguishable, suggesting that this criterion is not relevant to define subpopulations of MSCs.

### Introduction

Mesenchymal stromal cells (MSCs) are culture-expanded, plastic-adherent progeny derived from tissue-resident mesenchymal progenitors.[1–3] These cells are typically culture expanded in a two-dimensional culture system as a polyclonal population and may be cryobanked for future clinical use.[2] The most prevalent source of MSCs for veterinary clinical use is adipose tissue, followed by bone marrow and umbilical cord.[4,5] The relative merits of

[1]Division of Applied Veterinary Research, Center for Veterinary Medicine, U.S. Food and Drug Administration, Laurel, Maryland, USA.
[2]Micro/Nanofluidic BioMEMS Group, Department of Electrical Engineering and Computer Science, Massachusetts Institute of Technology, Cambridge, Massachusetts, USA.
[3]Office of New Animal Drug Evaluation, Center for Veterinary Medicine, U.S. Food and Drug Administration, Rockville, Maryland, USA.

availability and ease of isolation and expansion of MSCs from adipose tissue have led to the development of adipose-derived MSC (Ad-MSC)-based therapies for use in allogeneic unrelated recipients for an array of ailments.[4,6,7]

Clinically, the utility of MSCs lies in their ability to influence repair of damaged tissue, alter the inflammatory response, and affect the functionality of bystander innate and adaptive immune cells.[8–11] Clinical trials to evaluate the therapeutic potential of MSCs for tissue regeneration and anti-inflammatory action have been initiated based on encouraging data from preclinical work in animal models and *in vitro* studies.[12–17] These clinical trials have revealed a marked heterogeneity in outcomes, ranging from a complete cure to no clinical benefit.[14,16,17,18]

The dissonance between preclinical and clinical outcomes may be due to discrepancies in clinical trial design, dosage, and route of MSC administration.[13] In addition, diverse therapeutic targets, severity of disease, variations in MSC sources (both donor and tissue), and different manufacturing conditions such as priming with cytokines and different storage procedures, MSC dosage, and route of administration are challenges to translating the therapeutic promise of MSCs into clinical effectiveness.[12,13]

A limiting factor in the development of efficacious MSC-based therapies is that these cells are heterogeneous and subject to functional alterations based on processing and culture conditions.[19] Although MSC functional heterogeneity has been recognized, its effect on preclinical and clinical outcomes has not been fully investigated. A multitude of factors contribute to functional heterogeneity of MSCs, including differences in donor and tissue sources, as well as differences in manufacturing processes such as culture conditions, including density of plating, culture medium, media supplements like fetal bovine serum (FBS), presence of oxygen, inclusion of growth factors like cytokines, culture duration and degree of expansion, and the method of cryopreservation.[13] In addition, methods routinely used to isolate MSCs yield populations that exhibit heterogeneity in terms of morphology, growth rate, proliferation, differentiation, and potency in function-based assays.[20] Additionally, cell surface markers used to define MSCs do not relate phenotype to function.[3,20] Further characterization is necessary to determine whether MSC preparations used in clinical trials are similar in composition and biological function. Traditional approaches have verified the multipotency of MSCs through *in vitro* experiments that quantify MSC capacity to form clones and differentiate along multiple lineages.[13,14,21] These assessments are retrospective and assume different subpopulations of MSCs are functionally equivalent. Thus, there is a need for development of methods to identify MSC subpopulations of predictable potency without labeling or differentiating these cells. This study was undertaken to identify and characterize distinct subpopulations of canine MSCs.

Variation in size is observed in heterogeneous MSC populations.[20] Size can potentially serve as an indicator of cell function. Researchers have used methods that size separate cells to evaluate the effects of different cell diameters and how size relates to a given function.[20,22,23] Our hypothesis is that cell size is a predictor of function.

To test this, herein, we used a high-throughput, biophysical, label-free microfluidic sorting approach to separate subpopulations of canine Ad-MSCs based solely on their size for subsequent characterization, and to evaluate the impact of culture conditions on the functionality of these subpopulations. We found that a subpopulation of larger canine Ad-MSCs with a mean diameter of $18.6 \pm 0.3\,\mu m$ proliferate more slowly, senesce at earlier passages, and are inclined to form adipocytes compared with a subpopulation of smaller MSCs with a mean diameter of $15.3 \pm 0.4\,\mu m$. We also found that proliferation and differentiation characteristics of MSCs are largely influenced by culture conditions and time in culture. Even though larger and smaller MSC subpopulations are functionally distinct, immunophenotyping that is routinely used to characterize MSCs failed to discern these subpopulations. We demonstrate that labeling for MSC cell surface markers does not distinguish between these distinct subpopulations, suggesting that this criterion is not relevant to define different MSC subpopulations. Finally, there are significant differences in gene expression among these subpopulations, indicating heterogeneity based on MSC size. Altogether, this work provides a strategy for identifying functional subpopulations of MSCs that could facilitate manufacturing of quality cellular therapies through better understanding of functional heterogeneity.

## Method

### *Serum-containing medium*

Serum-based medium consisted of Dulbecco's modified Eagle's medium (DMEM) with low glucose (Catalog No. D5523; Sigma, St. Louis, MO) dissolved into tissue culture grade water (Catalog No. 17-724Q; Lonza, Walkersville, MD), filter sterilized, and supplemented with 4 mM GlutaMAX (Catalog No. 35050-061; Thermo Fisher Scientific, Pittsburgh, PA), 1× Antibiotic–Antimycotic (Catalog No. 15240-62; Thermo Fisher Scientific), and 10% heat-inactivated FBS (Catalog No. SH30070.03HI; HyClone, Logan, UT).

### *Serum-free medium*

Serum-free medium composition and its preparation was described in detail in our previous study.[24]

### *Donor animals*

Canine Ad-MSC donor specifications are listed in Table 1. The Center for Veterinary Medicine, Office of Research Institutional Animal Care and Use Committee (IACUC) approved the purchase of adipose tissue from BioreclamationIVT (Westbury, NY). In addition, the IACUC also approved the site of fat tissue collection and the amount of fat tissue. Donors were considered healthy based on physical examination reports, current vaccination records for rabies, distemper, parvo, parainfluenza, and canine adenovirus, and negative test results for heartworm disease and blood-borne pathogens, such as *Anaplasma*, *Babesia*, *Ehrlichia* spp., and *Borrelia*.

## Experiment

### *Culture of canine Ad-MSC*

About 50 g of canine subcutaneous adipose tissue from the abdominal area of six donors was purchased from BioreclamationIVT. The tissue samples were thoroughly

Table 1. Canine Adipose-Derived Mesenchymal Stromal Cell Donors

| *Animal number* | *Breed* | *Age (years)* | *Gender* | *Cell yield*[a] | *Experiment number* |
|---|---|---|---|---|---|
| Donor 1 | Beagle | 3.8 | Female | $4.47\times10^5$ | Figures 6 and 7 and Supplementary |
| Donor 2 | Beagle | 3.2 | Female | $0.93\times10^6$ | Figures S1, S4–S6 |
| Donor 3 | Beagle | 3.0 | Female | $0.68\times10^6$ | |
| Donor 4 | Beagle | 4.0 | Female | $1.12\times10^5$ | Figures 1–5 and Supplementary Figure S2 |
| Donor 5 | Beagle | 3.5 | Female | $1.10\times10^5$ | |
| Donor 6 | Beagle | 2.3 | Female | $0.68\times10^5$ | |

[a]Cell yield is per gram of adipose tissue.



rinsed with warm phosphate-buffered saline (PBS; Catalog No. 10010031; Thermo Fisher Scientific, Carlsbad, CA) containing 5% Antibiotic–Antimycotic solution (Catalog No. 15240062; Life Technologies, Carlsbad, CA). The tissue was placed in a sterile culture dish and minced with a scalpel into an enzymatic solution containing 500 CDU/mL of Type 4 collagenase (Catalog No. LS004188; Worthington, Lakewood, NJ). The enzymatic digestion was continued at 37°C. The reaction was stopped by adding DMEM containing 10% FBS when <5% of the initial tissue remained by visual examination. The mixture was allowed to separate at room temperature (RT) and the nonbuoyant fraction was collected into a fresh tube. Cells were collected by centrifugation at $400\times g$ for 5 min at RT. Collected cells were washed with PBS containing 2% Antibiotic–Antimycotic solution for a total of three washes. Cells were suspended in red cell lysis buffer (Catalog No. A1049201; Thermo Fisher Scientific, Pittsburgh, PA) and incubated on ice for 10 min to remove contaminating erythrocytes. Cells were separated from lysed erythrocytes by centrifugation at $400\times g$ for 5 min at RT. Cells were washed twice with PBS containing 2% Antibiotic–Antimycotic solution to remove traces of red cell lysis buffer. Cells were finally suspended into serum-containing or serum-free medium. Cell counts were determined using an automated cell counter. Cells were plated at a density of 30,000 cells/cm$^2$ and cultured in serum-containing or serum-free medium at 0.32 mL/cm$^2$. Two days later medium was replaced to remove unattached cells.

When well-developed colonies appeared, cells were harvested by trypsinization and suspended in 90% medium, in which they were cultured, supplemented with 10% DMSO (Catalog No. D8418; Sigma), and cryopreserved in liquid nitrogen. To assess cell viability, a vial was thawed rapidly in a 37°C water bath and recovered cells were diluted with 9 mL of serum-containing or serum-free medium, and centrifuged at $200\times g$ for 10 min at RT. Cell pellets were gently suspended in serum-containing or serum-free medium and cell viability and cell numbers were assessed after staining with Trypan Blue in an automated cell counter (Countess, Invitrogen, Carlsbad, CA). Cells were plated at a density of 30,000 cells/cm$^2$ in serum-containing or serum-free medium and these cells were designated as first passage (P1). Confluent ($\sim$ 80%) monolayers of MSCs were serially passaged to a maximum of three passages in serum-containing or serum-free medium.[25] The total number of times the MSCs in a given population doubled during culture were dependent on passage number. At P1, in serum-containing medium there were 1.6–2.2 population doublings (PDs), whereas in serum-free medium there were 2.2–2.6 PDs. The cumulative PDs up to passage 3 (P3) for MSCs in serum-containing medium were 4.1–6.3, whereas for MSCs in serum-free medium were 6.2–7.6.

### *Size-based sorting of canine Ad-MSCs*

Canine Ad-MSCs were sorted as a function of suspended cell diameter using a trapezoidal and spiral microfluidic channel (Fig. 1A). This inertial spiral microfluidic device was fabricated in polydimethylsiloxane (PDMS) using standard microfabrication soft lithographic techniques described previously.[26,27] The master mold with specific channel dimensions was designed using SolidWorks Software and then fabricated by micro milling machine (Whits Technologies, Singapore) on aluminum for PDMS casting. The PDMS replica was fabricated by molding degassed PDMS (mixed in a 10:1 ratio of base and curing agent, Sylgard 184; Dow Corning, Hayward, CA) on the mold and baking in the oven for 1 h at 90°C. The fluidic access holes were punched inside the device using Harris Uni-Core puncher (Catalog No. WHAWB100073; Sigma) and the device was irreversibly bonded to a thick layer of plain PDMS using a plasma machine (Harrick Plasma, Ithaca, NY). The assembled device was finally placed inside an oven at 70°C for 30 min to further enhance the bonding strength. The spiral microfluidic device was crafted such that it has a single inlet and two outlets and exhibited a trapezoidal cross-section of 80 μm inner depth, 130 μm outer depth, with an overall width of 600 μm (Fig. 1A). This device was designed for a high-throughput separation with separation speeds achieving as high as 0.35 million cells per minute.

Subconfluent canine Ad-MSCs from all six donors were harvested by trypsinization. Cells were suspended at 100,000 cells/mL in either serum-containing or serum-free medium. Suspended Ad-MSCs were then introduced into the microfluidic sorter with a PHD ultra infusion/withdrawal pump (Catalog No. 703006; Harvard Apparatus, Holliston, MA) at differing flow rates, initially at 3.5 mL/min (high flow rate) followed by 1.5 mL/min (low flow rate; Fig. 1B). These flow rates separate MSCs into different trajectories at different lateral positions along the sorter under the influence of inertial lift. Canine Ad-MSCs with broad size distribution were initially sorted at a higher flow rate to separate MSCs of larger diameter from the rest of the population and were collected at the inner outlet. Canine Ad-MSCs exiting the outer outlet were reintroduced into the sorter again at a lower flow rate to separate Ad-MSCs of smaller diameter and were collected at the outer outlet. Sorted cells were examined under a Nikon Eclipse Ti2 microscope both in suspension and

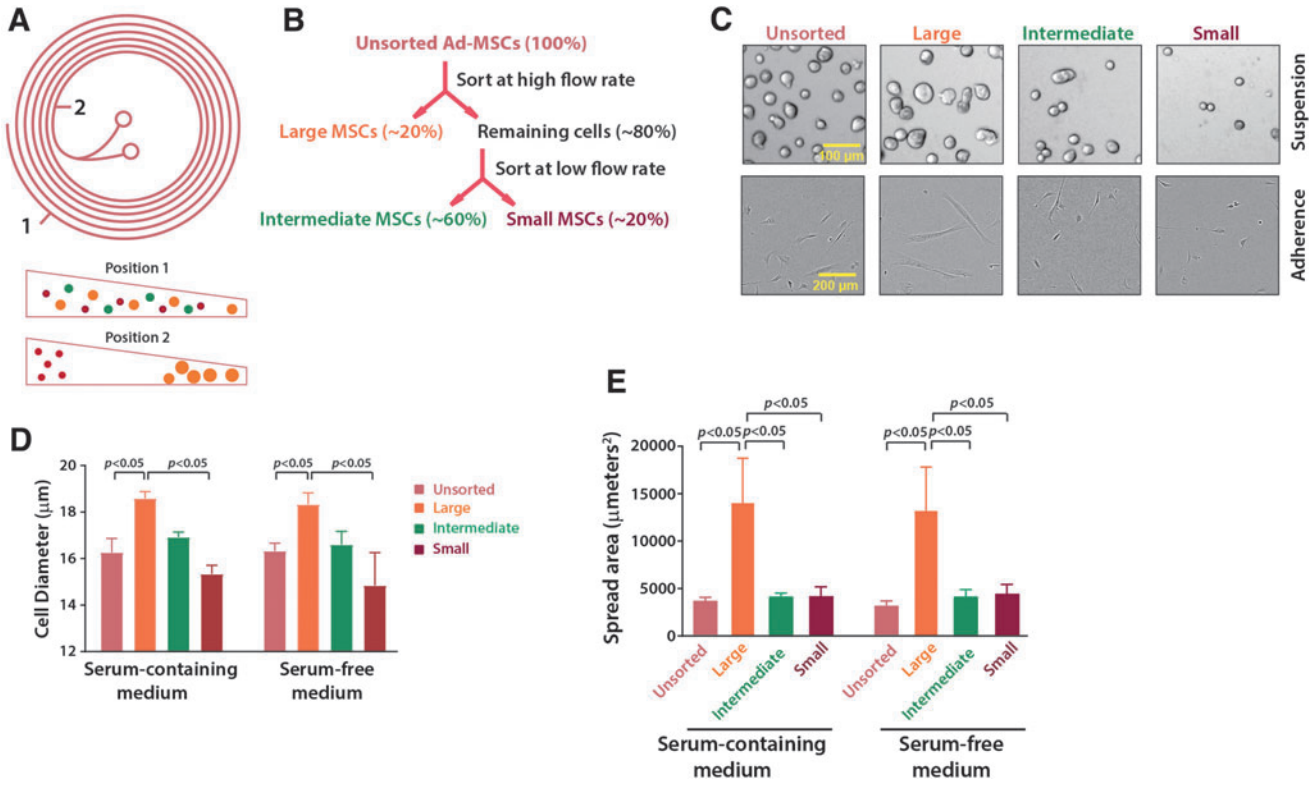


**FIG. 1.** Microfluidic-based size sorting of cultured canine Ad-MSCs. **(A)** *Top*, spiral microfluidic sorter. Suspended canine Ad-MSCs were pumped into the sorter at the inlet using a syringe pump and subpopulations of MSCs of differing diameter were obtained at the two outlets. *Bottom*, cross-sectional view of the sorter. Pumped MSCs travel spirally and during their path, cells are separated based on inertia, with MSCs of larger diameter traveling slowly and accumulating near the inner wall and MSCs of smaller diameter traveling faster on the outer wall. **(B)** Schematic for separation of MSCs based on size. **(C)** Suspended and adherent morphology of the resultant sorted canine Ad-MSCs from Donor 1 at P1 with varying diameter collected at the inner and outer outlets. **(D)** Suspended diameter of unsorted and sorted canine Ad-MSCs at P1. More than 20 cells each from Donors 4 to 6 were used to determine the mean diameter. **(E)** Cell spread area of unsorted and sorted canine Ad-MSCs Donor 2 at P1. Spread area was determined using the IncuCyte ZOOM live-cell imaging system. Data are expressed as mean ± SD, with $p < 0.05$ indicated. Ad-MSCs, adipose-derived mesenchymal stromal cells; P1, first passage; SD, standard deviation.

adherence to examine the success of separation. Cell-spread areas of unsorted and sorted Ad-MSCs were calculated using IncuCyte live-cell analysis imaging system (Essen Bioscience, Ann Arbor, MI).

### *Canine Ad-MSC proliferation assays*

Proliferation rates of canine Ad-MSCs were measured as previously described.[25] Proliferation of unsorted and sorted canine Ad-MSCs from Donors 4 to 6 was examined by analyzing the area occupied by cells (i.e., cell confluence) over time by IncuCyte Zoom based on area (confluence) metrics. Population doubling time (PDT) was calculated as previously described.[25] The extent of cell proliferation at different passages, expressed as *PD*, was calculated using the formula:

$$PD = \frac{[\log 10(N_H) - \log 10(N_1)]}{\log 10(2)}$$

where $N_H$ is the harvested cell number and $N_1$ is the plated cell number. At each passage, the *PDT*, was calculated using the formula:

$$PDT = \frac{[\log 10(2) \times t]}{[\log 10(N_H) - \log 10(N_1)]}$$

where $N_H$ is the harvested cell number and $N_1$ is the plated cell number. Cells were also observed under a Nikon Eclipse Ti2 microscope and photographed at defined intervals to document morphology.

### *Canine Ad-MSC colony-forming unit–fibroblast assay*

To determine the clonogenicity of canine Ad-MSCs, we size sorted MSCs at P1 and P3 from Donors 4 to 6 (see Table 1). Approximately 50 unsorted or sorted MSCs per well were plated in triplicate onto six-well plates (Corning, Rochester, NY) and cultured in either serum-containing or serum-free medium. Growth medium was replaced every 3 days. Colony-forming unit–fibroblast (CFU-F) colonies with at least 25 cells or >2 mm in diameter were visualized and enumerated following staining with Crystal Violet (0.5% solution; Catalog No. C0775; Sigma). CFU-F colonies were photographed using IncuCyte Zoom (Essen Bioscience).

### *Canine Ad-MSC senescence assay*

To assess the senescence of canine Ad-MSCs, we size sorted MSCs at P3 from Donors 4 to 6 (Table 1). Both unsorted and sorted MSCS were subjected to β-galactosidase staining using a kit from Cell Signaling Technologies (Danvers, MA) as per the manufacturer's instructions (Catalog No. 9860S). Stained cells were photographed using a Nikon Eclipse Ti2 microscope.

### *Canine Ad-MSC flow cytometry*

Unsorted and size-sorted canine Ad-MSCs at P3 from Donor 1 were incubated in a blocking solution containing in 1× PBS supplemented with 5% FBS. Cells were recovered by centrifugation and stained with anti-CD14 coupled to fluorescein isothiocyanate (FITC) (Catalog No. 557153, IgG2a, κ; BD Biosciences, La Jolla, CA), anti-CD34 coupled to phycoerythrin (PE) (Catalog No. 12-0340-42, IgG1; eBioscience, San Diego, CA), anti-CD44 coupled to FITC (Catalog No. 11-5440-42, IgG2a, κ; eBioscience), and anti-CD90 coupled to PE (Catalog No. 12-5900-42, IgG2b; eBioscience) antibodies or matching isotype controls as described previously.[25] After incubation in the dark, cells were washed twice with a wash buffer (1× PBS supplemented with 1% FBS and 0.1% sodium azide), resuspended in blocking solution and subjected to flow cytometry using FACS Jazz flow cytometer (BD biosciences) as described previously.[25] Data were analyzed with FlowJo Software (Ashland, OR).

### In vitro *canine Ad-MSC differentiation assays*

Trilineage (osteogenic, chondrogenic, and adipogenic) differentiation potential was evaluated for unsorted and size-sorted canine Ad-MSCs at P1. MSCs were cultured in serum-containing or in serum-free medium.

Osteogenic differentiation. Unsorted and size-sorted MSCs at P1 were seeded at 50,000 cells/well in duplicate in a 24-well plate. A day later, the growth medium in both cultures in half the wells was exchanged to DMEM containing FBS and in the remaining wells the growth medium was exchanged to osteogenic induction medium (low-glucose DMEM supplemented with 10% FBS; 100 units/mL of penicillin and 100 μg/mL streptomycin, Catalog No. P4333; 2 mM L-Glutamine, Catalog No. G7513; 100 nM Dexamethasone, Catalog No. D4902; 10 mM β-glycerophosphate, Catalog No. G9422; 50 μM L-ascorbic acid 2-phosphate, Catalog No. A8960—all from Sigma). Media in both groups of wells were completely replaced every 3 days. Cells were cultured for a total of 21 days before assessment of mineralization. Cells were washed once with PBS and fixed with 10% neutral buffered formalin (Catalog No. HT 500128; Sigma) for 5 min at RT. Residual formalin was removed by washing cells with water twice. Cells were stained with 2% Alizarin Red S (pH 4.2, Catalog No. A5533; Sigma) for 5 min at RT. Stained cells were then washed five times with water and staining was evaluated by light microscopy.

Chondrogenic differentiation. Unsorted and size-sorted MSCs at P1 were seeded at 250,000 cells per 15-mL test tube in duplicate. Cells were centrifuged at 1000 rpm for 5 min. Supernatant was removed. Cell pellets were either resuspended in DMEM containing FBS or chondrogenic induction medium (low-glucose DMEM supplemented with 100 units/mL of penicillin and 100 μg/mL streptomycin [Catalog No. P4333; Sigma]; 2 mM L-glutamine [Catalog No. G7513; Sigma]; 100 nM dexamethasone [Catalog No. D4902; Sigma]; 50 μM L-ascorbic acid 2-phosphate [Catalog No. A8960; Sigma]; 1% ITS-Premix [Catalog No. I3146; Sigma]; 1 mM sodium pyruvate [Catalog No. 11360070; Thermo Fisher Scientific, Pittsburgh, PA]; and 10 ng/mL human TGF-β1 [Catalog No. 240-B; R&D Systems, Minneapolis, MN]). Cells were centrifuged at 1000 rpm for 5 min for a second time then cultured without disturbing the cell pellet. Medium was replaced every 3 days for 21 days. Cells were washed with PBS, fixed with 10% neutral buffered formalin (Catalog No. HT 500128; Sigma), and stained with Toluidine Blue (Catalog No. T3260; Sigma). Staining was evaluated by light microscopy.

Adipogenic differentiation. Unsorted and size-sorted MSCs at P1 were seeded at 50,000 cells/well in duplicate in a 24-well plate. A day later, the growth medium in both cultures in half the wells was exchanged to DMEM-containing FBS and in the remaining wells the growth medium was exchanged to adipogenic induction medium (high-glucose DMEM supplemented with 100 units/mL of penicillin and 100 μg/mL streptomycin, Catalog No. P4333; 1 μM dexamethasone, Catalog No. D4902; 5% rabbit serum, Catalog No. R4505; 5 μM rosiglitazone, Catalog No. R2408, and 5 μM insulin, Catalog No. I9278—all from Sigma). Medium was replaced every 3 days for a total of 21 days. Cells were carefully washed with PBS, fixed with 10% neutral buffered formalin (Catalog No. HT 500128; Sigma) for 30 min at RT. Cells were washed once with 60% isopropanol before staining. The cells were incubated with 0.18% Oil Red O (Catalog No. O0265; Sigma) reagent for 10 min at RT. Excess stain was removed by washing with water. The cells were visualized under a Nikon Eclipse Ti2 microscope.

### *RNA sequencing*

Supplementary Figure S1 outlines the experimental strategy and the number of samples analyzed. Canine Ad-MSCs at P1 and P3 from Donors 1 to 3 were size sorted using microfluidics and the total RNA was extracted using the RNeasy Kit (Catalog No. 74104; Qiagen, Germantown, MD) as per the manufacturer's instructions. Genomic DNA was removed by treating total RNA with 25 units of DNAse I (Catalog No. 552598; BD Biosciences) at 37°C for 10 min. Total RNA was then recovered using the RNeasy Kit (Qiagen) as per the manufacturer's recommended procedure. The quantity and quality of the extracted RNA was determined using the NanoDrop Spectrophotometer (all samples had 260/280 values between 1.93 and 2.1) and Agilent 2100 Bioanalyzer (RNA integrity number ≥8; Agilent Technologies, Santa Clara, CA). The cDNA libraries were constructed using 4 μg of total RNA with the TruSeq Kit (Illumina, San Diego, CA), as per the manufacturer's instructions. The amplified cDNA fragments were then validated for 160 bp (15 SD) insert sizes using an Agilent 2100 Bioanalyzer. The final pooled library was diluted to

1.8 pmol before hybridization. Sequencing of the cDNA library was undertaken with the Illumina NextSeq 500 (Illumina) at $2 \times 75$ bp paired-end sequencing.

### *Reference-based mapping, assembly, and identification of differentially expressed genes*

The raw reads were mapped to the canine reference genome (CanFam 3.1.93; Ensembl) with default mapping options using CLC Genomics Workbench 10.1.1 (Qiagen, Redwood City, CA). The mapped reads were assigned to transcripts using the expectation-maximization estimation algorithm and Ensembl gene annotation (CanFam 3.1.93). The gene-level expression was calculated as the sum of transcript-level expression. The library sizes were subjected to the trimmed mean of M value normalization. The counts were then subjected to differential gene expression analysis using a generalized linear model. The genes with absolute $\log_2$-fold change >0.58, Benjamini–Hochberg (BH) false discovery rate (FDR) <0.05 and counts per million reads mapped (CPM) >0.50 in at least three samples were considered differentially expressed. The raw sequencing data will be available in NCBI Gene Expression Omnibus upon acceptance of the article.

### *Principal component analysis*

The principal component analysis (PCA) was performed using CLC Genomics Workbench (Qiagen). The log CPM values were mean centered and scaled to unit variance across samples for each gene. The genes with no expression across all samples were excluded from analysis.

### *Gene ontology analysis*

Gene ontology (GO) annotations comprising 16,763 genes and 116,050 gene sets were downloaded from Gene Ontology Consortium. GO enrichment analysis of the differentially expressed genes (DEGs) was performed using CLC Genomics Workbench (Qiagen). The GO terms were considered significantly enriched when BH-FDR < 0.05.

### *Gene set enrichment analysis*

The enrichment of the 50 Hallmark Gene Sets in the entire dataset was examined using gene set enrichment analysis (GSEA) as previously described.[28] We used $p < 0.01$ in combination with BH-FDR < 0.05 as criteria to identify the significantly enriched gene sets.

### *Statistical analysis*

Statistical analysis was performed using Graph Pad Prism Software (La Jolla, CA). For multiple comparisons, significance was determined using one-way analysis of variance followed by the Tukey's honest significant difference. Two-way comparison was performed using the Student's *t*-test. A *p*-value < 0.05 was considered significant.

## Experimental Results

### *Size-based sorting of canine Ad-MSCs*

Earlier reports indicated that proliferation and multipotency of MSCs may be dependent on size.[22,23] However, it is not clear whether media conditions also influence these size-based functional properties. To investigate this, we size separated canine Ad-MSCs cultured in serum-containing or serum-free medium using a fabricated inertial microfluidic device (Fig. 1A).[29] The spiral microfluidic channel has a straight inlet, and highly curved channels and two outlets (Fig. 1A). Canine Ad-MSCs entering into the channel initially experience a net lift because of wall-induced lift forces; however, as they travel through the spirals, they additionally experience drag forces called Dean vortices because of counter-rotating flows generated by curved channels. Both lift and drag forces are dependent on cell size and a combination of these forces shifts cells toward different equilibrium positions along the walls of the channels. In this way, smaller size cells are retained through the outer outlet, whereas larger size cells are retained through the inner outlet of the channel (Fig. 1A). Canine Ad-MSCs separated by this device retained a high viability (>90%). Thus, speed, quantity, and quality of separation provided by microfluidic device enabled us to perform further morphological, molecular, and biochemical characterization of size-sorted canine Ad-MSCs.

We performed size separation at both a high and a low flow rate to separate larger MSCs from the rest of the population (Fig. 1B). This approach propelled larger MSCs toward the inner wall region and directed smaller MSCs into the Dean's vortices at the outer wall region (Fig. 1A). This differential flow rate approach resulted in three distinct MSC subpopulations: In the first step at the high flow rate, the separation resulted in a population enriched in cells of larger mean diameter ($18.6 \pm 0.3$ μm for MSCs cultured in serum-containing medium and $18.3 \pm 0.5$ μm for MSCs cultured in serum-free medium) and a population depleted of these larger cells. In the second step at the low flow rate, the population depleted of larger cells is further separated into cells of smaller ($15.3 \pm 0.4$ μm for MSCs cultured in serum-containing medium and $14.8 \pm 1.4$ μm for MSCs cultured in serum-free medium) and an intermediate mean diameter ($16.9 \pm 0.2$ μm for MSCs cultured in serum-containing medium and $16.6 \pm 0.6$ for MSCs cultured in serum-free medium). Microscopy images of cells exiting from the microfluidic device further confirmed the existence of three subpopulations (Fig. 1C). Neither culture medium nor the donor source affected the heterogeneity in cell size because we detected similar size cells in all canine Ad-MSC samples (Fig. 1C, D and Supplementary Fig. S2). Optical imaging of adherent cells revealed a significantly greater number of large, flat, and irregularly shaped cells in the larger canine Ad-MSC subpopulation but not in the small or intermediate canine Ad-MSC subpopulations (Fig. 1C and Supplementary Fig. S2). To additionally confirm the size disparity, we evaluated the cell spread area of unsorted and sorted canine Ad-MSCs cultured in serum-containing or serum-free medium. In accordance with the data presented in Figure 1C and Supplementary Figure S2, we found that the spread area of canine Ad-MSCs is dependent on their size (Fig. 1E). Finally, we determined the percentages of each subpopulation of MSCs in total MSC population and found that large or small MSC subfractions constitute < 20% of the total cell population, whereas a vast majority of the MSCs falling under the intermediate subfraction (Supplementary

Fig. S3). In summary, the collected canine Ad-MSC subpopulations from the microfluidic device were distinctly different in size: larger MSCs and smaller MSCs.

### *Proliferation kinetics and stemness of sorted canine Ad-MSCs*

Studies with human MSCs have found that smaller MSCs proliferate more rapidly compared with larger MSCs.[30–33] To test whether size disparities also reflect the phenotype of canine Ad-MSCs, we examined the growth kinetics of unsorted and size-sorted cells. We found that larger canine Ad-MSC subpopulations proliferated more slowly compared with smaller Ad-MSC subpopulations in serum-containing medium (Fig. 2A). We previously demonstrated that canine Ad-MSCs cultured in serum-free medium proliferated more rapidly than those cultured in serum-containing medium.[24,25] In this study, we found that canine Ad-MSCs of all sizes cultured in serum-free medium proliferated at a similar rate as seen in our previous study, and there were no significant differences in proliferation rates based on size of the MSC population (Fig. 2A). Interestingly, smaller MSCs in serum-containing medium proliferate at a similar rate to MSCs of all sizes in serum-free medium (Fig. 2A).

Computation of PDT of different subpopulations of canine Ad-MSCs further confirmed that smaller MSCs proliferate faster than other subpopulations, as demonstrated by shorter PDT in both serum-containing and serum-free medium (Fig. 2B). However, in serum-free medium, we observed that PDT of large and intermediate-sized cells is shorter, when compared with serum-containing medium, whereas the PDT of smaller cells is similar in both media (Fig. 2B). Combined, the results of Figure 2 suggest that the canine Ad-MSC growth phenotype is both dependent on size and culture medium.

To further define the functional properties of canine Ad-MSC subpopulations, we initially analyzed their CFU-F ability. In general, time in culture affects CFU-F ability, with canine Ad-MSCs from earlier passages forming more colonies compared with later passages regardless of size and culture medium (Fig. 3). However, in accordance with our previous findings, we found that CFU-F ability of unsorted Ad-MSCs is higher in serum-free medium compared with serum-containing medium (Fig. 3A, B).[25] Additionally, CFU-F ability of smaller Ad-MSCs is higher compared with larger Ad-MSCs only in serum-containing medium but not in serum-free medium (Fig. 3A, B). Canine Ad-MSCs of all sizes yielded similar number of colonies in serum-free medium (Fig. 3B). These results taken together with the results of Figure 2 suggest that canine Ad-MSC phenotype is dependent on size and culture medium.

### *Senescence of sorted canine Ad-MSCs*

Senescence of canine Ad-MSCs in culture is inevitable and culture medium has a significant influence on the onset of this process.[25] Senescent cells undergo irreversible growth arrest but continue to be metabolically active, develop a large, flat morphology, and exhibit senescence-associated β-galactosidase activity.[34,35] We investigated

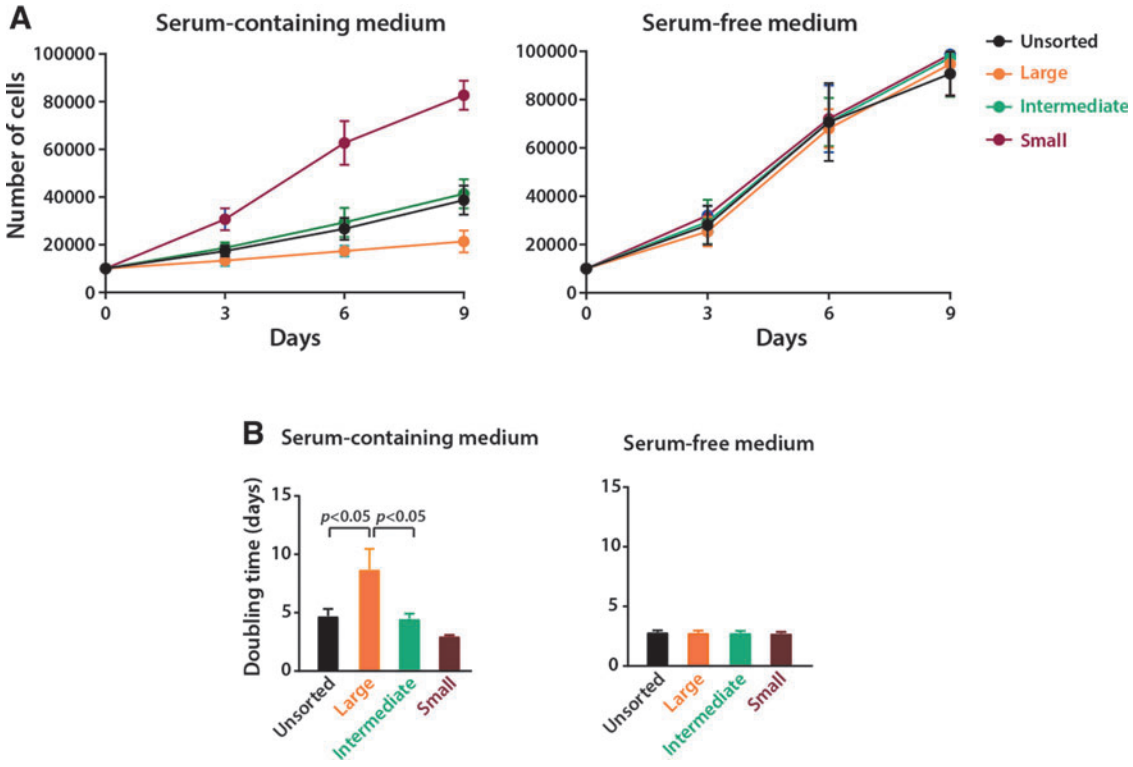


**FIG. 2.** Proliferation kinetics and PDT of size-sorted canine Ad-MSCs at P1 in serum-containing or serum-free medium from a representative donor (Donor 4). **(A)** *Left*, proliferation of unsorted and sorted MSCs in serum-containing medium. *Right*, proliferation of unsorted and sorted MSCs in serum-free medium. **(B)** Average for canine Ad-MSCs in serum-containing or serum-free medium. Data are expressed as mean ± SD (three replicates). PDT, population doubling time.

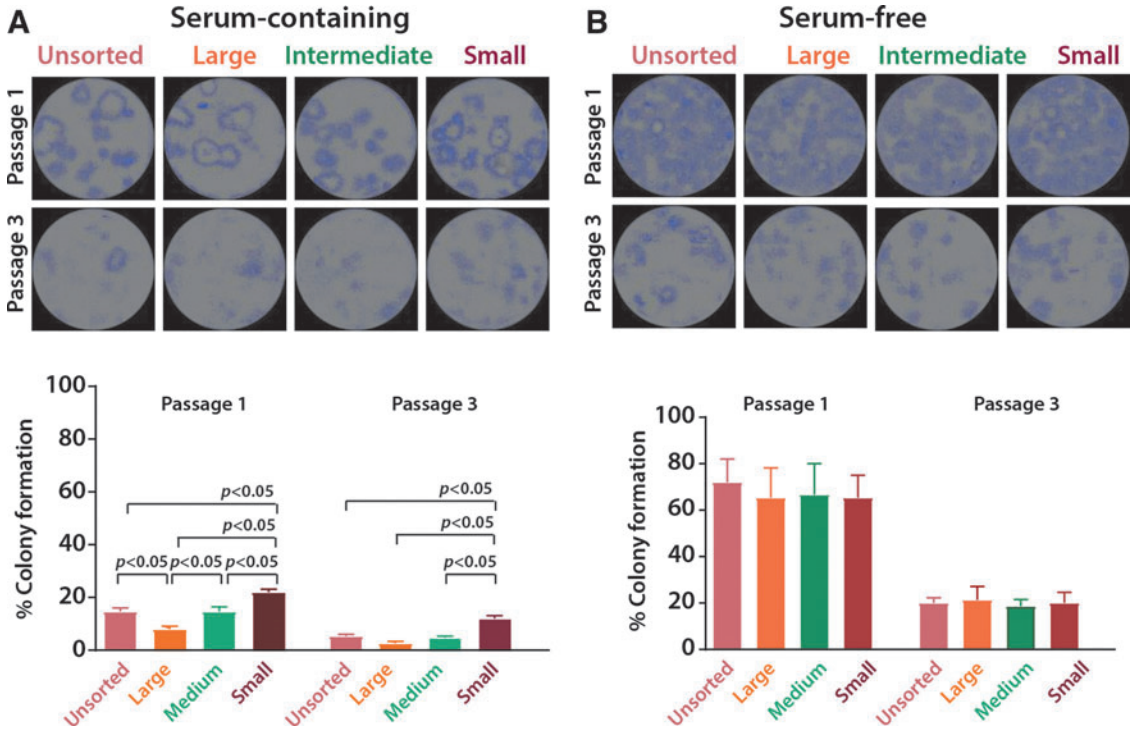


**FIG. 3.** Enumeration of colony formation by unsorted and size-sorted canine Ad-MSCs. CFU-F of unsorted and sorted canine Ad-MSCs serially passaged in serum-containing medium **(A)** or serum-free medium **(B)**. Canine Ad-MSCs from Donors 4 to 6 were isolated and expanded up to P3 in serum-containing or serum-free medium and were tested for CFU-F formation. *Top*, whole plate images of stained colonies for cells from all three donors at P1 and P3. 4× magnification. *Bottom*, colony-forming efficiency of canine Ad-MSCs cultured in serum-containing or serum-free medium expressed as the ratio of number of colonies to the number of initial inoculum. Data are expressed as mean ± SD (three replicates). CFU-F, colony-forming unit-fibroblast; P3, passage 3.

each subpopulation of canine Ad-MSCs to evaluate senescence at P3 in both culture media. We found that larger canine Ad-MSC subpopulations undergo senescence compared with smaller canine Ad-MSC subpopulations (Fig. 4A). In addition, culture of canine Ad-MSCs in serum-containing medium accelerates the onset of senescence as demonstrated by a higher number of β-galactosidase-positive cells (Fig. 4B). Thus, an early onset of senescence in larger canine Ad-MSCs may, in part, explain their slower proliferation rate when cultured in serum-containing medium.

### *Multipotency of sorted canine Ad-MSCs*

To further define the importance of cell size in assessing the multipotentiality of each category of canine Ad-MSC subpopulations, cells were analyzed for multilineage differentiation potential. Differentiation positivity was determined by optical imaging following chemical induction of differentiation along adipogenic, chondrogenic, and osteogenic lineages. We found that all subpopulations of canine Ad-MSCs remained multipotent. However, we found that serum cultures of larger subpopulations of canine Ad-MSCs are more inclined to form adipocytes compared with smaller subpopulations (Fig. 5). In contrast, all categories of subpopulations of canine Ad-MSCs in serum-free medium showed no differences in staining pattern along multilineages. Thus, it appears that larger canine Ad-MSCs are more adipogenic in serum-containing medium compared with other subsets of canine Ad-MSCs. These results suggest that both cell size and culture medium may influence the differentiation potential, as well as functional aspects of canine Ad-MSCs.

### *Immunophenotyping of size-sorted canine Ad-MSCs*

The International Society for Cellular Therapy (ISCT) has established a common set of markers to qualify cells as human MSCs.[3] To examine the possibility that these consensus markers may identify different subpopulations of canine Ad-MSCs, we performed flow cytometry analysis with antibodies specific for these cell surface antigens. In accordance with our previous findings, we found that unsorted canine Ad-MSCs stained positive for CD44 and CD90 (*THY1*; Fig. 6).[36] Interestingly, staining patterns and staining intensity of all subpopulations of canine Ad-MSCs were similar to unsorted cells (Fig. 6). Thus, these results suggest that consensus MSC surface markers do not identify distinct subpopulations of canine Ad-MSCs.

### *RNA sequencing of different subpopulations of MSCs*

Cell size as a marker for MSC function does not obviate the potential for additional biomolecular markers that may correlate size with phenotype. Therefore, to identify such molecular markers that are associated with cell size, we performed RNA sequencing. In addition, we also evaluated the effect of the culture medium, passage number, and donor variation on the transcriptome of distinct subpopulations of canine Ad-MSCs.

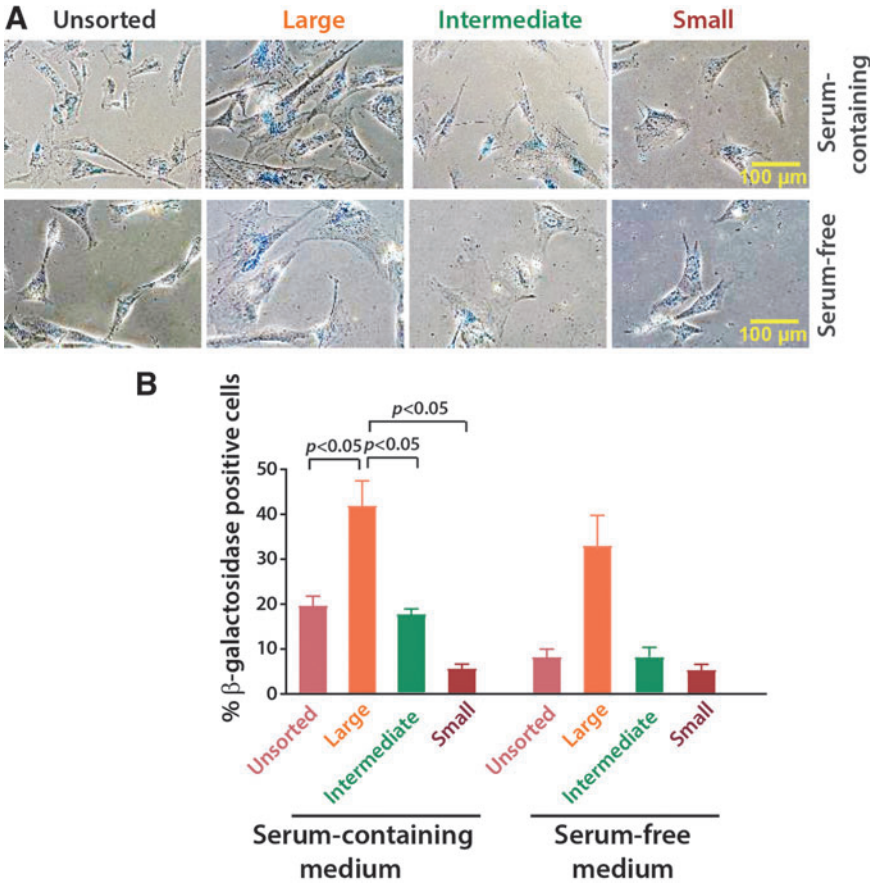


**FIG. 4.** Senescence of unsorted and size-sorted canine Ad-MSCs cultured in serum-containing or serum-free medium. **(A)** β-galactosidase staining of cultured canine Ad-MSCs at P3 from a respresentive donor (Donor 4). 20× magnification. **(B)** Quantification of β-galactosidase-positive cells. Data are expressed as mean ± SD (three replicates).



An average of 13.6 million read pairs per sample were generated that aligned to the canine reference genome. To determine whether the gene expression profiles were different among the three subpopulations of canine Ad-MSCs, we performed the PCA. Data in Figure 7A show how gene expression profiles cluster based on culture media conditions over the two principal components, which together represent a 29.8% variation. PCA indicated tighter clustering between subpopulations of canine Ad-MSCs cultured in either media type regardless of culture time (Fig. 7A). However, the presence or absence of serum seems to affect the PCA pattern in these samples (Fig. 7A). Thus, the cell culture media appear to influence gene expression more than cell size (Fig. 7A). We additionally performed PCA analysis for various subgroups, which again showed clustering of genes based on the passage of MSCs culture medium used to grow MSCs and MSC cell size (Supplementary Fig. S4). Volcano plots displaying log fold change against the noise-adjusted/standardized signal ($-\log_{10}$ *p*-value) further confirmed that DEGs are different based on the passage of MSCs, culture medium used to grow MSCs or MSC cell size (Supplementary Fig. S5).

To identify the genes contributing to the expression profiles associated with media, passage, and cell size, we performed differential gene expression analysis using an additive model (Supplementary Fig. S1). Results are provided in Supplementary Excel File. We found that the fold change of differential gene expression correlates with cell size (Supplementary Fig. S6). For example, the fold change of a downregulated gene was greater in larger MSCs compared with smaller MSCs (Supplementary Fig. S6).

We next set out to identify DEGs between small and large canine Ad-MSCs cultured in serum-containing medium or serum-free medium at two passages. We identified 2 upregulated and 64 downregulated genes across all comparisons (Fig. 7B). We found that cyclin-dependent kinase inhibitor 1A (*CDKN1A*), a 21 kDa Cyclin/Cyclin-Dependent Kinase (Cdk) inhibitor that blocks cell cycle progression from $G_1$ to S phase and modulates cellular senescence,[37] is upregulated in large MSCs compared with small MSCs. Processing of genes for their associated molecular function and biological processes by GO enrichment analysis showed that the top-ranked biological processes in serum-based cultures of small MSCs at P3 were associated with DNA binding or DNA metabolism (Supplementary Fig. S7A). Conversely, the top-ranked biological processes were negative regulation of cellular and biological processes in serum-free cultures of unsorted MSCs at P3 (Supplementary Fig. S7C). Combined, these results may in part explain the senescent phenotype and proliferation attenuation of canine Ad-MSCs at higher passages (Fig. 4).[34]

GSEA, using the Hallmark gene set collection,[28] identified significantly enriched functional groups ($p < 0.05$) altered by cell size, culture medium, or time in culture (Fig. 7C). We found that a set of genes whose collective function is to promote cell growth [mechanistic target of rapamycin 1 (mTORC1) signaling] and cell proliferation

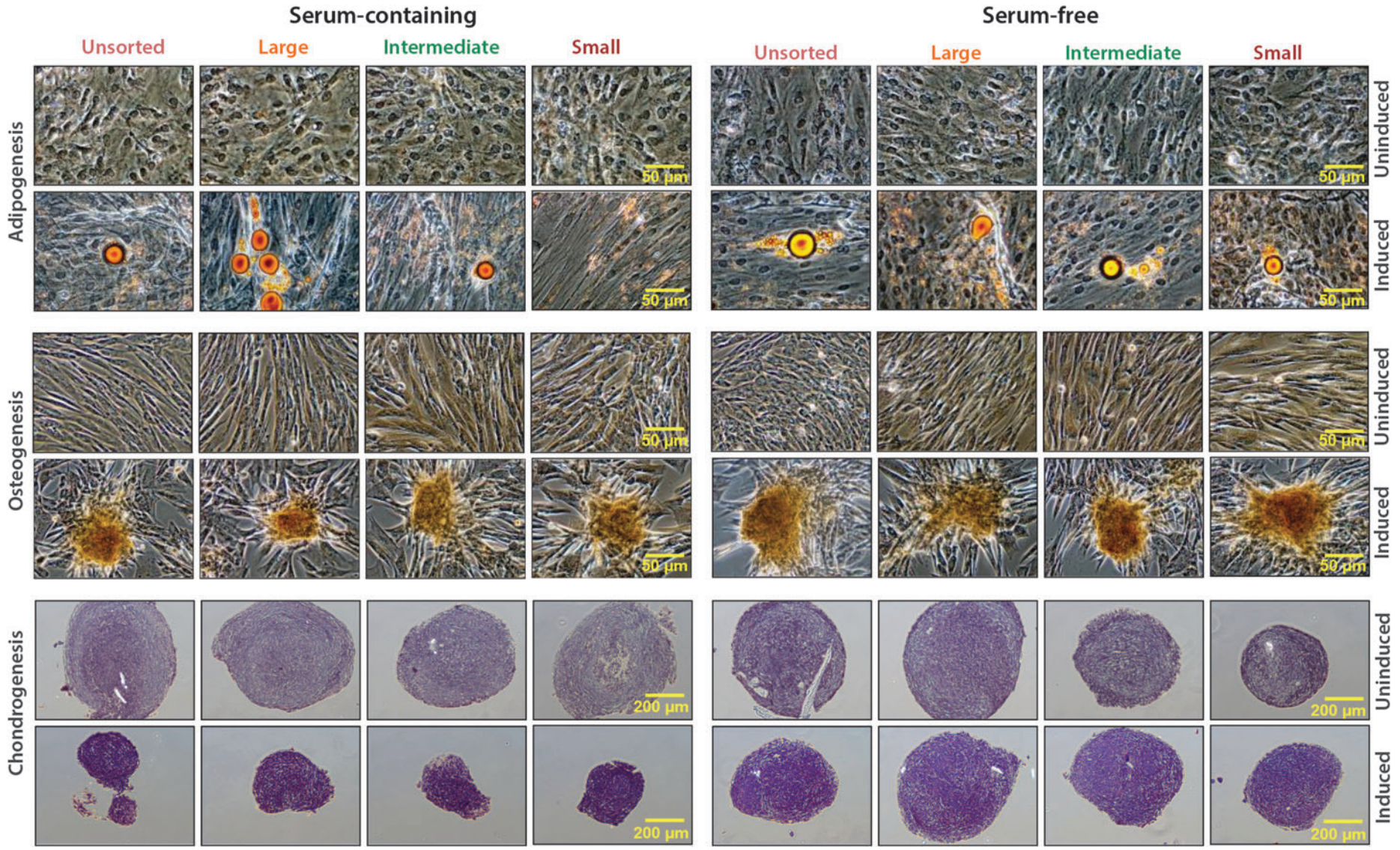


**FIG. 5.** Trilineage differentiation of unsorted and size-sorted canine Ad-MSCs at P1. *Top*, adipogenic potential of unsorted and sorted canine Ad-MSCs from a representative donor (Donor 4) in both types of culture media was assessed with Oil Red O staining after 21 days of induction/maintenance. Uninduced cells maintained their characteristic spindle-shaped morphology. Upon induction, canine Ad-MSCs cultured in both media types formed adipocytes with intracellular lipid droplets (20×magnification). *Middle*, osteogenic potential of unsorted and sorted canine Ad-MSCs from a representative donor in both cultures was assessed with Alizarin Red staining after 21 days of induction. Canine Ad-MSCs cultured in both media types formed calcified cell aggregates (20×magnification). *Bottom*, chondrogenic potential of unsorted and sorted canine Ad-MSCs from a representative donor (Donor 4) in both culture media was assessed with Toluidine Blue staining at 21 days postinduction (10×magnification).

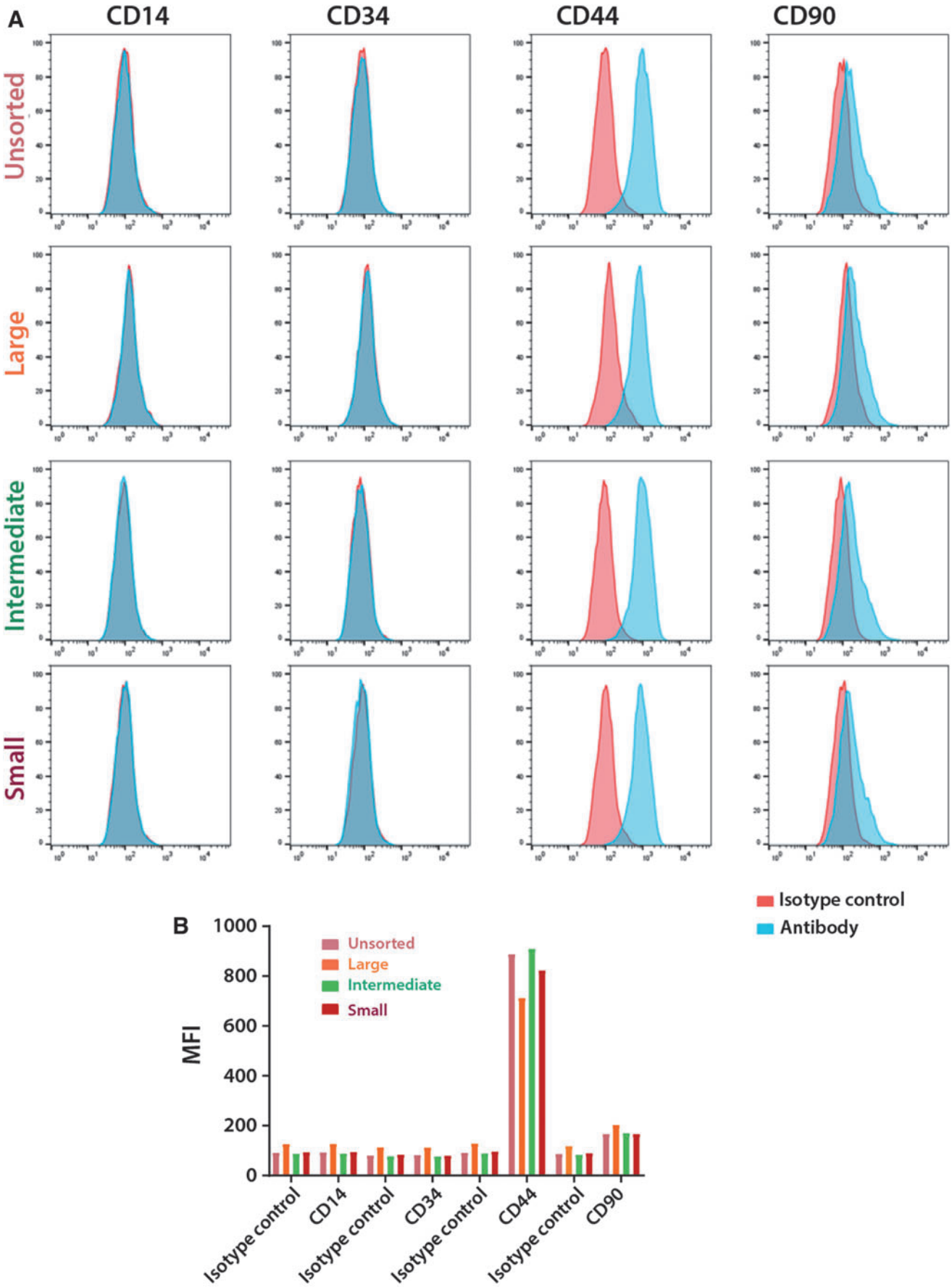


**FIG. 6.** Immunophenotyping of unsorted and size sorted canine Ad-MSCs in serum-containing medium at P3. **(A)** Representative diagrams showing FACS analysis for canine Ad-MSCs from one donor (Donor 1). *Red line* indicates isotype matching antibody-stained cells. *Cyan shade* indicates antigen-specific antibody-stained cells. **(B)** MFI detected by surface antigen antibodies was calculated. FACS, fluorescence activated cell sorting; MFI, median fluorescence intensity.

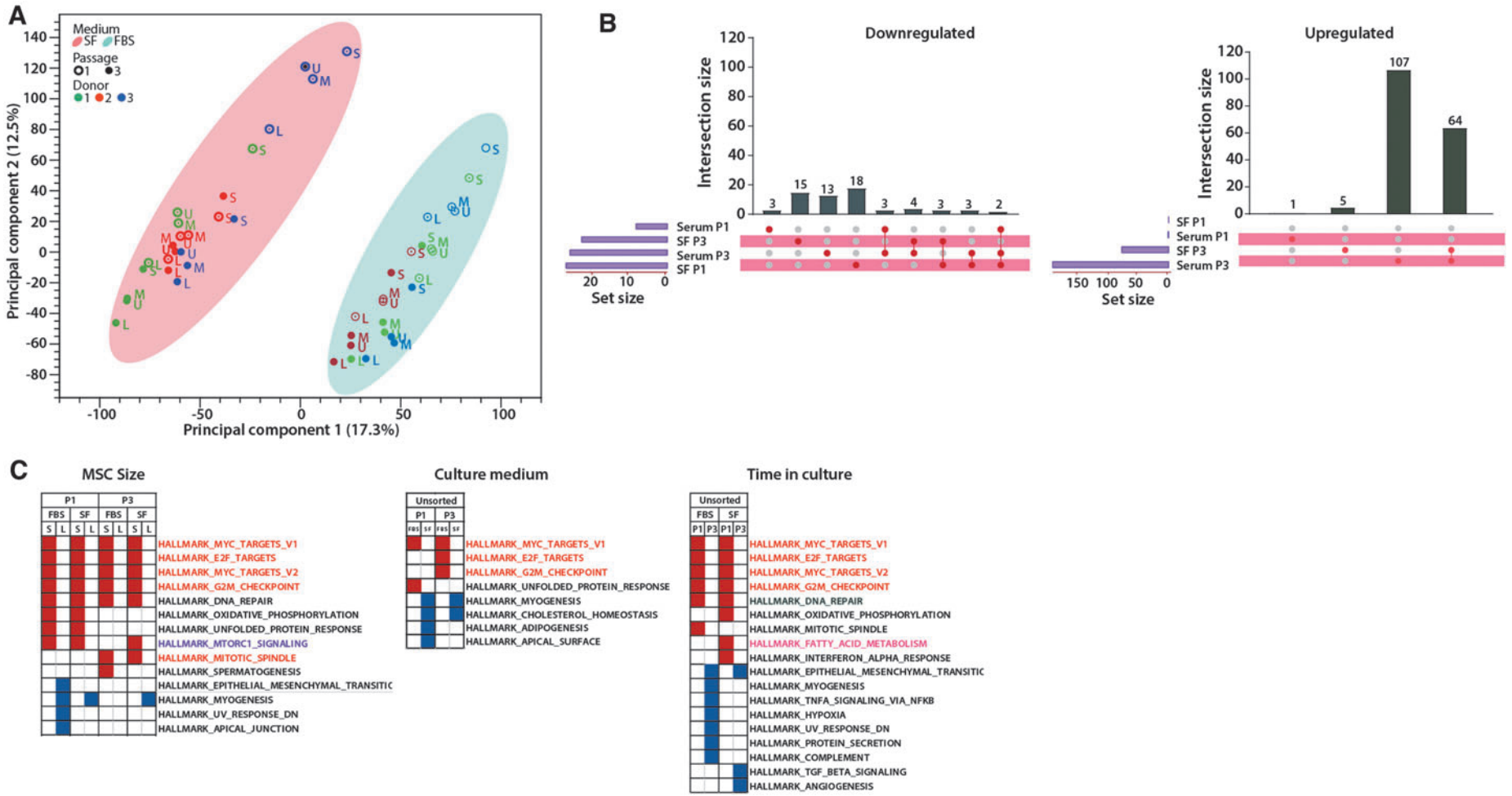


**FIG. 7.** RNA sequencing of unsorted and size sorted canine Ad-MSCs from Donors 1 to 3. **(A)** PCA analysis of genes differentially expressed between MSC subpopulations cultured in serum-containing or serum-free medium at P1 and P3. Nearly one third of the variation in gene expression across all samples is captured by the first two principal components (PC1 and PC2). **(B)** UpSet plot of downregulated (*left*) and upregulated genes (*right*) in smaller MSCs compared with larger MSCs cultured in serum-containing or serum-free medium at indicated passages. The *top* bar graph summarizes the number of DEGs for each unique or overlapping combination. The *bottom left* horizontal bar graph (set size) shows the number of DEGs in each treatment group. The *circles* in each panel's matrix are either empty (*Gray*) suggesting that this set is not part of that intersection or filled (*red*) suggesting that this set is part of that intersection. Connected *circles* indicate intersection of DEGs between treatment groups. **(C)** Representative functional groups enriched for DEGs. The genes which were differentially expressed in larger and smaller MSCs (*left*), in MSCs cultured in serum-containing or serum-free medium (*middle*) or in MSCs at P1 and P3 (*right*) comparisons were determined using Hallmark gene set tool. Enriched functional groups (BH-FDR <0.05) were identified for each comparison and groups representative of overall enrichment results for each comparison are shown. BH, Benjamini–Hochberg; DEGs, differentially expressed genes; FDR, false discovery rate; PCA, principal component analysis.

[myelocytomatosis (*myc*) targets, *e2f* targets] are enriched in small MSCs compared with large MSCs, thus confirming their faster growth and proliferation kinetics (Figs. 2, 4, and 7C). For all cell sizes regardless of culture medium, we found that genes involved in cell proliferation were upregulated at earlier passages (Fig. 7C). We also found that genes involved in fatty acid metabolism are elevated in canine Ad-MSCs in a culture medium- and passage number-dependent manner (Fig. 7C). Taken together, these results suggest that the transcriptome analysis of canine Ad-MSCs reflects their culture expansion (enrichment of cell growth, cell proliferation, and DNA repair genes) and their intrinsic fate (enrichment of fatty acid metabolism genes).

## Discussion

MSC heterogeneity with respect to morphology, size, growth and proliferation, differentiation potential, passage number, and manufacturing process, is well established and recognized.[19,20,38] It is likely that this heterogeneity contributes to variability in clinical outcomes. In addition to cellular functional heterogeneity, in an allogeneic setting, the preconditioning of MSCs, injection protocol, cell dose, carrier solution, freeze/thaw conditions, degree of mismatch of major histocompatibility antigens, and donor/recipient gender mismatch are also contributors to clinical outcomes.[13,39] For some applications involving heterogeneous samples, such as peripheral blood mononuclear cells, the specific functional subpopulations are well known and characterized; however, this extent of knowledge does not exist for MSCs. An understanding of MSC heterogeneity and the specific functionality of subpopulations may lead to improved consistency in clinical outcomes for MSC-based therapeutic products. To address this unmet need, we utilized microfluidics to isolate and study different subpopulations of MSCs. We evaluated the effect of cell culture media and cell size to characterize the MSCs. We then compared the characterization data for each subpopulation with their intrinsic biological functions.

A microfluidics-based separation of cells offers several advantages over other cell separation methods, such as flow cytometry. A microfluidics-based separation of cells requires no prior knowledge of cell surface proteins and does not alter the cellular phenotype, both of which are important considerations when separating cells by flow cytometry. Inertial microfluidics utilize a combination of hydrodynamic forces dependent on particle size to separate cells in a continuous flow within the channel. The control of movement of particles is based on hydrodynamic forces derived from the channel structure and size of the particles without the need for active force fields. Therefore, inertial microfluidics are fast, simple, and cost-effective devices for the separation of particles or cells based on size. Assuming having a homogenous cell size is important, this methodology represents a significant advancement in terms of analyzing heterogeneous cell populations because this approach can be applied to MSCs sourced from different donors and manufactured under different conditions.

We observed cell size differences in culture-expanded canine Ad-MSCs regardless of the culture medium. We found that proliferation of canine Ad-MSCs is dependent on size. The smaller, fibroblast-like MSCs proliferate faster but reduced in proportion of the total cells with successive passages that gave rise to larger, senescent MSCs. We also found that these size-dependent functions of canine Ad-MSCs are influenced by culture medium. For instance, size-dependent growth characteristics were evident only in serum-based medium but not in serum-free medium. Serum-dependent differences in growth properties for human MSCs have been reported. Human bone marrow-derived MSCs cultured in FBS-containing medium senesced rapidly.[40] However, supplementation with either platelet lysate or growth factors such as fibroblast growth factor (FGF) or platelet derived growth factor (PDGF) delayed the onset of senescence in human MSCs.[41–43] Our serum-free medium contains both FGF and PDGF. Therefore, for this reason, the onset of senescence in MSCs is delayed when grown in serum-free medium and, as a result, all subpopulations of canine Ad-MSCs are in replicative stage. However, this rejuvenation advantage is lost when canine Ad-MSCs are cultured in serum-containing medium. Although we did not examine, size separation of canine Ad-MSCs at later passages (P5 and beyond) would have enabled us to discern the growth differences among all three subpopulations of canine Ad-MSCs in serum-free medium.

Most importantly, a criterion for the identification of human MSCs is the expression of specific cell surface markers did not identify different subpopulations of canine MSCs in our experiments. Therefore, this criterion may not be relevant for the identification of functionally heterogeneous subpopulations of canine Ad-MSCs. Nonetheless, human MSCs expressing distinct surface markers display different biological properties, therefore making it possible to isolate functionally distinct human MSCs based on surface markers.[44] However, the expression of these markers and their utility to identify functionally different subpopulations in canine Ad-MSCs are currently unknown. Finally, age and gender of the MSC donor also contribute to variations in canine MSC biology.[45] In this study, we tested Ad-MSCs from young female dogs, so the contribution of age and gender to MSC heterogeneity was not evaluated.

The size of the cells within an adult tissue reflects their growth and proliferation rates, which are controlled by intrinsic programs and the levels of extracellular growth factors.[46,47] In addition, other factors such as nutrient levels and mechanical signals can impinge on these pathways positively or negatively.[48] The availability of nutrients in the environment is one of the factors that determines the biomass of the cells. Most terminally differentiated cells in a tissue are uniform in size. However, progenitor cells, such as MSCs, which give rise to these differentiated cells are heterogeneous in size and the *in vivo* significance of size heterogeneity is not known.[19] Differences in size may be attributed to their growth stage and cell cycle status. The best-characterized cell growth pathway is the IGF/PI3K/AKT/mTORC1 pathway. mTORC1 is a central mediator of the signal from insulin-like growth factor (IGF) through PI3K/AKT to biogenic pathways.[49–51] The mTORC1 pathway is a major regulator of cell growth and plays a critical role in regulating cell size, particularly in promoting the increase in cell size upon activation.[52] mTORC1 also integrates inputs from other major cues such as stress, energy status, oxygen, and amino acid levels into cell growth, and thus acts as a signaling node at which energetic and stress signals can modulate growth factor signaling. Enhanced signaling through

the mTORC1 pathway promotes multiple biogenic processes such as nutrient uptake, protein and lipid biosynthesis, promotion of biogenesis, and inhibition of catabolic pathways such as autophagy.[51] In addition to its direct effect on cell growth, the mTORC1 pathway also contributes to cell size homeostasis by activating a potent negative feedback loop through insulin receptor substrate to negatively regulate signaling by the IGF receptor.[51] We found that genes in the mTORC1 pathway are upregulated in smaller MSCs but not in larger MSCs. We also found that a set of genes (see Fig. 7C and Supplementary Excel File) whose collective function is to promote cell proliferation, are also upregulated in smaller MSCs. Thus, upregulation of genes that control both cell growth and proliferation in smaller MSCs may explain their rapid growth in serum-containing medium.

Adipose tissue is active and highly dynamic, expanding and shrinking in response to various physiological and nutritional stimuli.[53] Expansion of adipose tissue could involve adipocyte hyperplasia or hypertrophy, the former highlighting the involvement of the stem cell component. Based on the results detailed in this report, we propose that the continued expression of *mTORC1* and other genes involved in cell cycle and cell proliferation drive both growth and proliferation of smaller MSCs culminating in hypertrophied and aged larger MSCs (Fig. 8). Several observations raise this possibility: first, larger MSCs proliferate at a slower rate; second, larger MSCs display a senescent phenotype, because of overexpression of *CDKN1A*, a potent inhibitor of cyclin kinases[37]; third, larger MSCs are inclined to form more differentiated adipocytes; and finally, senescence of cells due to hyperactivity of mTORC1 is also reported in other adult stem cells.[54] Because the mTORC1 pathway directly links nutrient uptake to cell growth and proliferation, the progression to large size is a successive process involving multiple intermediate cell sizes. We observe intermediate cell sizes in our sorted subpopulation (Fig. 8). Taken together, these results suggest that the smaller MSCs are of a proliferating phenotype and larger MSCs are of a differentiating phenotype. The larger MSCs may replace aging or damaged adipocytes, which further suggest that Ad-MSCs are intrinsically fated to become adipocytes.

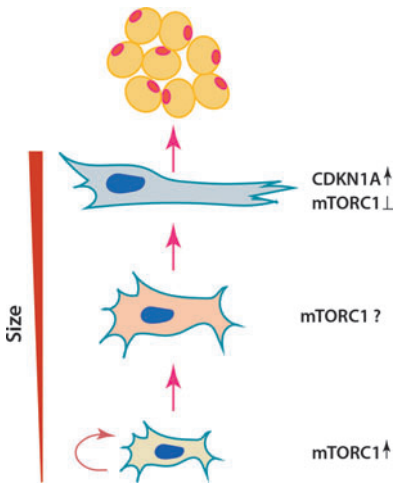


**FIG. 8.** Proposed model for canine Ad-MSCs role. Activation of genes that link nutrient uptake to cell growth such as *mTORC1*, may drive the growth of canine Ad-MSCs resulting in a hypertrophied phenotype. mTORC1, mechanistic target of rapamycin 1 (mTORC1).

Standardization of measurements has been recognized as one of the most significant challenges facing clinical transition of MSC-based therapies and collaborative efforts from academia, industry, and government stakeholders have attempted to address this issue.[55] Established consensus markers for identification of human MSCs do not relate phenotype to function for canine Ad-MSCs, and thus lack predictive value for cell functionality.[3,20] As part of this work, we presented a strategy for separating functionally distinct subpopulations of MSCs that could serve as part of a platform for comparing the functional capacity of MSCs manufactured by different processes.

In addition to their intrinsic role as a source of adipocytes, MSCs also display adaptive functions. Stimulated MSCs are known to secrete a host of paracrine molecules that act on target cells to exert anti-inflammatory, immunomodulatory, or proangiogenic effects.[13] However, knowledge regarding how these wide-ranging activities of MSCs are exhibited within specific populations of MSC is not yet known. While it is true that the functional attributes of MSCs may be evoked in response to extracellular cues, it is unlikely that these responses are homogeneous at the MSC populational level. This gap in scientific understanding of the functional aspects of MSCs presents challenges to correlating a specific subpopulation of MSCs with a specific therapeutic effect.

Functional heterogeneity is significant for both understanding and clinical transition of MSC biology. This recognized heterogeneity needs to be mitigated or differences in culture expanded MSCs need to be exploited to improve clinical outcomes. Successful clinical transition requires a large number of homogeneous population of MSCs with predictable efficacy to improve the clinical outcome. The potential for increased effectiveness of size-sorted MSCs has been demonstrated. For instance, it was found that larger subpopulations of human bone marrow-derived MSCs improved recovery of lethally irradiated mice as compared with unsorted or heterogeneous MSCs.[56] Therefore, the microfluidics method of separation described in this report, or perhaps other methods of separating desired populations of MSCs can be used to manage heterogeneity of MSCs. We found that smaller MSCs have the greatest potential to replicate, which limits the time required for scaling. In addition, these rapidly dividing smaller MSCs are more effective in terms of self-renewal and secreting paracrine factors than endogenous tissue progenitors residing in stromal vascular fraction (SVF).[57,58] The residing progenitors are at resting stage and exhibit different transcriptional profiles than actively proliferating culture-adapted MSCs.[59] Therefore, smaller MSCs may be superior to SVF in terms of achieving therapeutic efficacy. Thus, separating these smaller MSCs from other cell types may improve the therapeutic outcomes. However, it remains to be determined whether smaller MSCs are also more potent than other subpopulations of MSCs for any or all their elicited functions. Predicting the potency of manufactured MSCs is difficult due to the lack of specific markers or assays that relate phenotype to function. Further evaluation of the functionality of size-separated MSCs, may lead to methods for identifying subpopulations of MSCs with desired therapeutic effects.

## Conclusions

In this study, we tested our hypothesis that cell size is a predictor of function. We used a high-throughput, biophysical, label-free microfluidic sorting approach to separate subpopulations of canine Ad-MSCs based solely on their size for subsequent characterization, and to evaluate the impact of culture conditions on the functionality of these subpopulations. We found that larger subpopulation of canine Ad-MSCs proliferate more slowly, senesce at earlier passages, and are inclined to form adipocytes compared with a subpopulation of smaller MSCs. We also found that proliferation and differentiation characteristics of MSCs are largely influenced by culture conditions and time in culture. Even though larger and smaller MSC subpopulations are functionally distinct, immunophenotyping that is routinely used to characterize MSCs failed to discern these subpopulations. Finally, there are significant differences in gene expression among these subpopulations, indicating heterogeneity based on MSC size. These results suggest that different subpopulations of MSCs have specific properties.

## Authors' Contributions

J.H. and D.Y. developed the microfluidic device. L.R.D. and Z.L. designed experiments. Z.L., L.R.D., and R.S. performed experiments and analyzed the data. L.R.D., M.J.M., and L.B. wrote the article.

## Disclaimer

The views expressed in this article are those of the authors and do not necessarily reflect the official policy of the Department of Health and Human Services, the U.S. Food and Drug Administration, or the U.S. Government.

## Acknowledgments

The authors wish to thank the CVM Stem Cell Tech team for many helpful suggestions and comments. The authors thank Alexis Norris, Division of Animal Bioengineering and Cellular Therapies, Office of New Animal Drug Evaluation, CVM for expert technical assistance on RNA-seq analysis.

## Disclosure Statement

No competing financial interests exist.

## Funding Information

This work was supported in part by a Challenge Grant from the office of the Chief Scientist and research funds from the Division of Applied Veterinary Research, Center for Veterinary Medicine, FDA.

## Supplementary Material

Supplementary Excel File
Supplementary Figure S1
Supplementary Figure S2
Supplementary Figure S3
Supplementary Figure S4
Supplementary Figure S5
Supplementary Figure S6
Supplementary Figure S7

## References

1. Caplan, A.I. Mesenchymal stem cells: time to change the name! Stem Cells Transl Med **6,** 1445, 2017.
2. Le Blanc, K., and Davies, L.C. MSCs—cells with many sides. Cytotherapy **20,** 273, 2018.
3. Dominici, M., Le Blanc, K., Mueller, I., *et al.* Minimal criteria for defining multipotent mesenchymal stromal cells. The International Society for Cellular Therapy position statement. Cytotherapy **8,** 315, 2006.
4. Marx, C., Silveira, M.D., and Nardi, N.B. Adipose-derived stem cells in veterinary medicine: characterization and therapeutic implications. Stem Cells Dev **24,** 803, 2015.
5. Sultana, T., Lee, S., Yoon, H.-Y., and Lee, J.I.K. Current status of canine umbilical cord blood-derived mesenchymal stem cells in veterinary medicine. Stem Cells Int **2018,** 8329174, 2018.
6. Devireddy, L.R., Boxer, L., Myers, M.J., Skasko, M., and Screven, R. Questions and challenges in the development of mesenchymal stromal/stem cell-based therapies in veterinary medicine. Tissue Eng Part B Rev **23,** 462, 2017.
7. Fortier, L.A., and Travis, A.J. Stem cells in veterinary medicine. Stem Cells Res Ther **2,** 9, 2011.
8. Shi, Y., Wang, Y., Li, Q., *et al.* Immunoregulatory mechanisms of mesenchymal stem and stromal cells in inflammatory diseases. Nat Rev Nephrol **14,** 493, 2018.
9. Le Blanc, K., and Davies, L.C. Mesenchymal stromal cells and the innate immune response. Immunol Lett **168,** 140, 2015.
10. Carrade, D.D., and Borjesson, D.L. Immunomodulation by mesenchymal stem cells in veterinary species. Comp Med **63,** 207, 2013.
11. Taechangam, N. Iyer, S.S., Walker, N.J., Arzi, B., and Borjesson, D.L. Mechanisms utilized by feline adipose-derived mesenchymal stem cell to inhibit T lymphocyte proliferation. Stem Cell Res Ther **10,** 188, 2019.
12. Borregowda, S.V., and Phinney, D.G. Therapeutic applications of mesenchymal stem cells. Biodrugs **26,** 201, 2012.
13. Galipeau, J., and Sensebe, L. Mesenchymal stromal cells: clinical challenges and therapeutic opportunities. Cell Stem Cell **22,** 824, 2018.
14. Martin, I., Galipeau, J., Kessler, C., Le Blanc, K., and Dazzi, F. Challenges for mesenchymal stromal cell therapies. Sci Transl Med **11,** eaat2189, 2019.
15. Phinney, D.G., Galipeau, J., Krampera, M., Martin, I., Shi, Y., and Sensebe, L. MSCs: science and trials. Nat Med **19,** 812, 2013.
16. Hoffman, A.M., and Dow, S.W. Stem cell trials using companion animal disease models. Stem Cells **34,** 1709, 2016.
17. Quimby, J.M., and Borjesson, D.L. Mesenchymal stem cell therapy in cats. Current knowledge and future potential. J Feline Med Surg **20,** 208, 2018.
18. Sacchetti, B., Funari, A., Remoli, C., *et al.* No identical ''mesenchymal stem cells'' at different times and sites: human committed progenitors of distinct origin and differentiation potential are incorporated as adventitial cells in microvessels. Stem Cell Reports **14,** 897, 2016.
19. Phinney, D.G. Functional heterogeneity of mesenchymal stem cells: implications for cell therapy. J Cell Biochem **113,** 2806, 2012.
20. Marklein, R.A., Lam, J., Guvendiren, M., Sung, K.E., and Bauer, S.R. Functionally-relevant morphological profiling:

a tool to assess cellular heterogeneity. Trends Biotechnol **36,** 105, 2018.
21. Mastrolia, I., Foppiani, E.M., Murgia, A., *et al.* Concise review: challenges in clinical development of mesenchymal stromal/stem cells. Stem Cells Transl Med **8,** 1135, 2019.
22. Gonzalez-Cruz, R.D., Fonseca, V.C., and Darling, E.M. Cellular mechanical properties reflect the differentiation potential of adipose-derived mesenchymal stem cells. Proc Natl Acad Sci U S A **109,** E1523, 2012.
23. Lee, W.C., Shi, H., Poon, Z., *et al.* Multivariate biophysical markers predictive of mesenchymal stromal cell multipotency. Proc Natl Acad Sci U S A **111,** E4409, 2014.
24. Devireddy, L.R., Myers, M., Screven, R., and Boxer, L. A serum-free medium formulation efficiently supports isolation and propagation of canine adipose-derived mesenchymal stem/stromal cells. PLoS One **14,** e0210250, 2019.
25. Liu, Z., Screven, R., Myers, M., and Devireddy, L.R. Characterization of canine adipose-derived mesenchymal stem/stromal cells in serum-free medium. Tissue Eng Part C Methods**24,** 399, 2018.
26. Warkiani, M.E., Tay, A.K., Guan, G., and Han, J. Membrane-less microfiltration using inertial microfluidics. Sci Rep **5,** 11018, 2015.
27. Ryu, H., Choi, K., Qu, Y., Kwon, T., Lee, J.S., and Han, J. Patient-derived airway secretion dissociation technique to isolate and concentrate immune cells using closed-loop inertial microfluidics. Anal Chem **89,** 5549, 2017.
28. Liu, Z., Petersen, R.B., and Devireddy, L.R. Impaired neutrophil function in 24p3 null mice contributes enhanced susceptibility to bacterial infections. J Immunol **190,** 4692, 2013.
29. Kwon, T., Yao, R., Hamel, J.-F.P., and Han, J. Continuous removal of small nonviable suspended mammalian cells and debris from bioreactors using inertial microfluidics. Lab Chip **18,** 2826, 2018.
30. Colter, D.C., Sekiya, I., and Prockop, D.J. Identification of a subpopulation of rapidly self-renewing and multipotential adult stem cells in colonies of human marrow stromal cells. Proc Natl Acad Sci U S A **98,** 7841, 2001.
31. Prockop, D.J., Sekiya, I., and Colter, D.C. Isolation and characterization of rapidly self-renewing stem cells from cultures of human marrow stromal cells. Cytotherapy **3,** 393, 2001.
32. Russell, K.C., Phinney, D.G., Lacey, M.R., Barrilleaux, B.L., Meyertholen, K.E., and O'Connor, K.C. In vitro high-capacity assay to quantify the clonal heterogeneity in trilineage potential of mesenchymal stem cells reveals a complex hierarchy of lineage commitment. Stem Cells **28,** 788, 2010.
33. Smith, J.R., Pochampally, R., Perry, A., Hsu, C., and Prockop, D.J. Isolation of a highly clonogenic and multipotential subfraction of adult stem cells from bone marrow stroma. Stem Cells **22,** 823, 2004.
34. Turinetto, V., Vitale, E., and Giachino, C. Senescence in human mesenchymal stem cells: functional changes and implications in stem cell-based therapy. Int J Mol Sci **17,** E1164, 2016.
35. Wagner, W., Bork, S., Horn, P., *et al.* Aging and replicative senescence have related effects on human stem and progenitor cells. PLOS One **4,** e5846, 2009.
36. Screven, R., Kenyon, E., Myers, M.J., *et al.* Immunophenotype and gene expression profile of mesenchymal stem cells derived from canine adipose tissue and bone marrow. Vet Immunol Immunopathol **161,** 21, 2014.
37. Georgakilas, A.G., Martin, O.A., and Bonner, W.M. p21: a two-faced genome guardian. Trends Mol Med **23,** 310, 2017.
38. Whitfield, M.J., Lee, W.C., and Van Vliet, J.J. Onset of heterogeneity in culture-expanded bone marrow stromal cells. Stem Cell Res **11,** 1365, 2013.
39. Pittenger, M.F., Discher, D.E., Peault, B.M., Phinney, D.G., Hare, J.M., and Caplan, A.I. Mesenchymal stem cell perspective: cell biology to clinical progress. NPJ Regen Med **4,** 22, 2019.
40. Duggal, S., and Brinchmann, J.E. Importance of serum source for the in vitro replicative senescence of human bone marrow derived mesenchymal stem cells. J Cell Physiol **226,** 2908, 2011.
41. Griffiths, S., Baraniak, P.R., Copland, I.B., Nerem, R.M., and McDevitt, T.C. Human platelet lysate stimulates high passage and senescent human multipotent mesenchymal stromal cell growth and rejuvenation in vitro. Cytotherapy **12,** 1469, 2013.
42. Cheng, Y., Lin, K.-H., Young, T.-H., and Cheng, N.-C. The influence of fibroblast growth factor 2 on the senescence of human adipose-derived mesenchymal stem cells during long-term culture. Stem Cells Transl Med **9,** 518, 2020.
43. Zhang, J.-M., Feng, F.-E., Wang, Q.-M., *et al.* Platelet-derived growth factor-BB protects mesenchymal stem cells (MSCs) derived from immune thrombocytopenia patients against apoptosis and senescence and maintains MSC-mediated immunosuppression. Stem Cells Transl Med **5,** 1631, 2016.
44. Mo, M., Wang, S., Zhou, Y., Li, H., and Wu, Y. Mesenchymal stem cell subpopulations: phenotype, property and therapeutic potential. Cell Mol Life Sci **73,** 3311, 2016.
45. Kresic, N., Simic, I., Lojkic, I., and Bedekovic, T. Canine adipose derived mesenchymal stem cells transcriptome composition alterations: a step towards standardizing therapeutic. Stem Cells Int **2017,** 4176292, 2017.
46. Bjorklund, M., and Marguerat, S. Determinants of cell size. Front Cell Dev Biol **5,** 115, 2017.
47. Amodeo, A.A., and Skotheim, J.M. Cell-size control. Cold Spring Harb Perspect Biol **8,** a019083, 2016.
48. Conlon, I.J., Dunn, G.A., Mudge, A.W., and Raff, M.C. Extracellular control of cell size. Nat Cell Biol **3,** 918, 2001.
49. Sabatini, D.M. Twenty-five years of mTOR: uncovering the link from nutrients to growth. Proc Natl Acad Sci U S A **114,** 11818, 2017.
50. Weichhart, T. mTOR as a regulator of life span, aging, and cellular senescence: a mini-review. Gerontology **64,** 127, 2018.
51. Saxton, R.A., and Sabatini, D.M. mTOR signaling in growth, metabolism, and disease. Cell **168,** 960, 2017.
52. Fingar, D.C., Salama, S., Tsou, C., Harlow, E., and Blenis, J. Mammalian cell size is controlled by mTOR and its downstream targets S6K1 and 4EBP1/eIF4E. Genes Dev **16,** 1472, 2002.
53. Gesta, S., Tseng, Y.H., and Kahn, C.R. Developmental origin of fat: tracking obesity to its source. Cell **131,** 242, 2007.
54. Gan, B., and DePinho, R.A. mTORC1 signaling governs hematopoietic stem cell quiescence. Cell Cycle **8,** 1003, 2009.

55. Simon, C.G., Lin-Gibson, S., Elliott, J.T., Sarkar, S., and Plant, A.L. Strategies for achieving measurement assurance for cell therapy products. Stem Cells Transl Med **5,** 705, 2016.
56. Poon, Z., Lee, W.C., Guan, G., *et al.* Bone marrow regeneration is promoted by biophysically sorted osteoprogenitors from mesenchymal stromal cells. Stem Cells Transl Med **4,** 56, 2015.
57. Gimble, J.M., Bunnell, B.A., Chiu, E.S., and Guilak, F. Concise review: adipose-derived stromal vascular fraction cells and stem cells. Let's us not get lost in the translation. Stem Cells **29,** 749, 2011.
58. Marklein, R.A., Klinker, M.W., Drake, K.A., Polikowsky, H.G., Lessey-Morillon, E.C., and Bauer, S.R. Morphological profiling using machine learning reveals emergent subpopulations of interferon- γ-stimulated mesenchymal stromal cells that predict immunosuppression. Cytotherapy **21,** 17, 2019.
59. Bourin, P., Bunnell, B.A., Casteilla, L., *et al.* Stromal cells from adipose tissue-derived stromal vascular fraction and culture expanded adipose tissue-derived stromal/stem cells: a joint statement of the International Federation for Adipose Therapeutics and Science (IFATS) and the International Society for Cellular Thearpy (ISCT). Cytotherapy **15,** 641, 2013.

Address correspondence to:
*Laxminarayana R. Devireddy, DVM, PhD*
*Division of Applied Veterinary Research*
*Center for Veterinary Medicine*
*U.S. Food and Drug Administration*
*8401 Muirkirk Road*
*Laurel, MD 20708*
*USA*

*E-mail:* Laxminarayana.Devireddy@fda.hhs.gov

*Received: April 7, 2021*
*Accepted: June 17, 2021*
*Online Publication Date: August 19, 2021*